

# Switchable diode effect and ferroelectric resistive switching in epitaxial BiFeO<sub>3</sub> thin films

Can Wang, Kui-juan Jin,<sup>a)</sup> Zhong-tang Xu, Le Wang, Chen Ge, Hui-bin Lu, Hai-zhong Guo, Meng He, and Guo-zhen Yang

Beijing National Laboratory for Condensed Matter Physics, Institute of Physics, Chinese Academy of Sciences, Beijing 100190, People's Republic of China

(Received 14 February 2011; accepted 20 April 2011; published online 10 May 2011)

Current-voltage hysteresis and switchable rectifying characteristics have been observed in epitaxial multiferroic BiFeO<sub>3</sub> (BFO) thin films. The forward direction of the rectifying current can be reversed repeatedly with polarization switching, indicating a switchable diode effect and large ferroelectric resistive switching. With analyzing the potential barriers and their variation with ferroelectric switching at the interfaces between the metallic electrodes and the semiconducting BFO, the switchable diode effect can be explained qualitatively by the polarization-modulated Schottky-like barriers. © 2011 American Institute of Physics. [doi:10.1063/1.3589814]

BiFeO<sub>3</sub> (BFO) is an extensively studied multiferroic material due to its potential device applications and interesting physics. Choi *et al.*<sup>1</sup> recently reported a switchable diode and photovoltaic effect in BFO *bulk single crystals*. The polarized BFO *crystals* show diodelike rectifying characteristics, and the direction of the diode can be switched by polarization reverse, which has been connected to the polarization-related asymmetry of impurity potentials.<sup>1</sup> The switchable diode behavior in BFO *crystal* has also been explained by a polarization-dependent depletion layer containing positive charged oxygen vacancies<sup>2</sup> or asymmetrical trap distributions.<sup>3</sup> Actually, the switchable diode effect has been rarely reported before and the mechanism behind the switchable diode effect remains unclear. However, resistive switching or conduction modulation induced by ferroelectric polarization has been revealed in more ferroelectric films<sup>4–7</sup> and ferroelectric tunneling junctions.<sup>8,9</sup> Most of the polarization modulated conduction behaviors have been related to the variation of potential barrier or depletion layer with polarization in the ferroelectrics.<sup>10–12</sup> The resistive switching controlled by ferroelectric polarization is called ferroelectric resistive switching, which is intriguing for the potential application in a nondestructive readout ferroresistive random access memory.

In this letter, we present the switchable diode effect and the ferroelectric resistive switching in epitaxially BFO *thin films*. BFO thin films were grown on SrRuO<sub>3</sub> (SRO)-covered SrTiO<sub>3</sub> (001) single crystals by pulsed laser deposition, using a XeCl 308 nm excimer laser with an energy density of ~1.5 J/cm<sup>2</sup> and a repetition rate of 2 Hz. The oxygen pressure was 10 Pa during the deposition and the substrate temperature determined by an infrared pyrometer was around 610 °C. X-ray diffraction patterns and transmission electron microscopy images (not shown here) indicate that the BFO thin films have been grown epitaxially without impurity phase. Pt dots in a diameter of 100 μm were grown on the BFO thin films as top electrode. The as-grown capacitance without poling by external high electrical field is denoted as virgin state in this letter. Leakage currents were measured

using computer-controlled Keithley meters with a delay time of 0.2 s for reading a current value. Ferroelectric hysteresis loops were measured on the capacitance configuration using Radiant ferroelectric tester Premier II.

Figure 1(a) shows the current-voltage (I-V) curves measured on the 240 nm BFO thin films. The numbers in the figure denote the sequence of voltage sweeps. The measurements were performed with 25 cycles by sweeping the bias voltage of the top electrode from 8 to -7.5 V and back to 8 V, repeatedly. The I-V curves in Fig. 1(a) show distinct hysteresis behavior, indicating a large resistive switching. Moreover, in the inset of Fig. 1(a), two I-V segments in the range of ±5 V are plotted using solid circle symbols and open circle symbols, respectively. The curve by the solid circles shows an obvious diodelike rectifying I-V characteristic, indicating a forward diode behavior, and the curve by the open circles indicates a reverse diode behavior. It can be seen that during a measuring cycle the diode polarity can be switched at around ±6 V. If a higher dc bias is applied, local joule heating will be un-negligible and may result in unre-

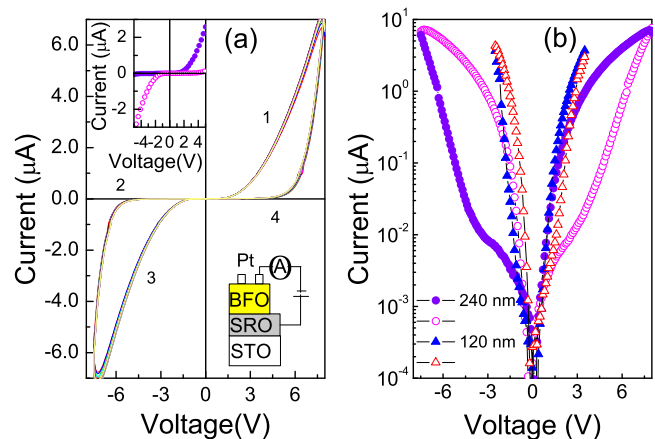


FIG. 1. (Color online) (a) I-V curves measured on a 240 nm BFO thin film; Insets show the sketch of the set up for the I-V measurements and I-V curves at the voltage range of ±5 V, which indicate the forward and reverse diode characteristics. (b) I-V curves for the 240 and 120 nm BFO films plotted on semilogarithmic scales. The curves by open symbols were measured on forward sweep (from negative to positive voltages), and the curves by solid symbols were measured on reverse sweep (from positive to negative voltages).

<sup>a)</sup> Author to whom correspondence should be addressed. Electronic mail: kjjin@aphy.iphy.ac.cn.

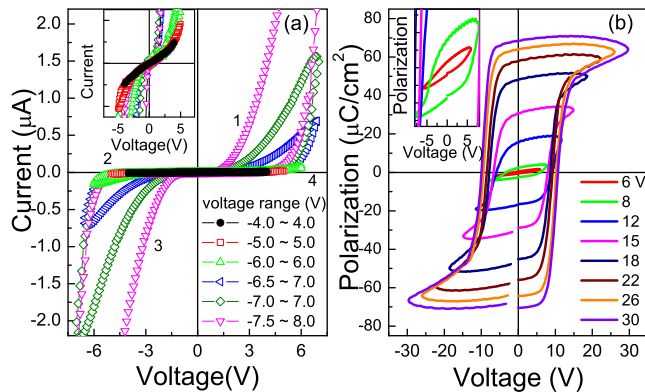


FIG. 2. (Color online) (a) I-V curves measured on a virgin BFO thin film by increasing the voltage sweep range. Inset shows a magnification of the I-V curves for low voltage range. (b) Ferroelectric loops measured at 50 kHz with various voltages (6–30 V). Inset shows that the ferroelectric loop starts to appear at around  $\pm 6$  V.

coverable behavior, so we cannot obtain I-V curve at higher dc voltages; however, a high-voltage short pulse is feasible to switch the polarization.

Figure 1(b) shows the I-V curves plotted on semilogarithmic scales for the 240 and 120 nm BFO films. The switchable diode behavior and resistive switching are also observed for the 120 nm film, where the applied voltage range is smaller around  $\pm 3$  V, meeting the requirement of small operation voltage for memory devices. In addition, the resistance switching ratio is 103 at  $-3$  V for the 240 nm films and it is 79 at  $-1$  V for the 120 nm films. It is worthy of mention that the observed ferroelectric resistance switching behavior in our BFO thin films would be different with that observed in some ferroelectric tunneling junctions,<sup>8,9</sup> because the tunneling current can only be taken into account for the ultrathin ferroelectric films, not for our films with the thickness of hundreds of nanometers.

In order to investigate the relation between the current hysteresis and ferroelectric polarization, we have measured I-V curves [shown in Fig. 2(a)] on a virgin 240 nm BFO film capacitance by increasing the sweep range step by step. At the beginning, the sweep voltage is in the range of  $\pm 4$  V and the I-V curve is almost symmetric and without hysteresis [as seen in the inset of Fig. 2(a)]. Then, as the voltage range is to  $\pm 6$  V, obvious hysteresis can be observed. With further increasing voltage range, the hysteresis becomes significantly large, and the diodelike behavior can be observed clearly. Contrastively, Fig. 2(b) shows the ferroelectric loops for the film measured at 50 kHz with various voltages, indicating that the film exhibits good ferroelectricity, and it is shown that the ferroelectric loop starts to appear at around  $\pm 6$  V. Though the coercive voltage may vary with measured frequency, the current hysteresis can be closely related with the ferroelectric polarization. For a virgin BFO capacitance, at low sweep voltage, there is no current hysteresis behavior related to the virgin state; however, the current hysteresis and diodelike rectifying behavior can be observed in an electrically poled BFO capacitance. It is indicated that the current hysteresis and diodelike behavior can be triggered and switched at high applied field, which can drive the ferroelectric domain switching.

Moreover, electrical pulses have been used to induce the variation of the ferroelectric state in the BFO capacitance. As shown in Figs. 3(a)–3(c), the conduction behaviors in a

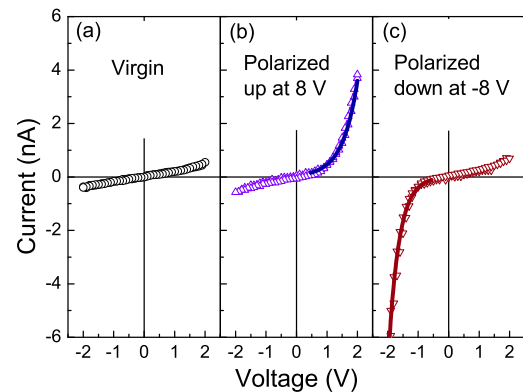


FIG. 3. (Color online) I-V curves of the SRO/BFO/Pt capacitance measured at (a) virgin state; (b) polarized up state; (c) polarized down state. The solid lines indicate an exponential fitting.

sweep voltage of  $\pm 2$  V have been measured on a SRO/BFO/Pt capacitance at three different situations that are virgin, polarized up at a square pulse of 8 V for 200 ms and polarized down at a square pulse of  $-8$  V for 200 ms, respectively. For the virgin state, the current is very small and increases linearly with voltage at both positive and negative bias; however, for the polarized up state, the current increases exponentially with positive voltage but increases slowly with negative voltage, which indicating a forward diodelike behavior; whereas, for the polarized down state, the current shows a reverse diode behavior. This result confirms again that the switchable diode behavior can be observed and it is controlled by the ferroelectric polarization.

The large leakage current in BFO has been attributed to the presence of oxygen vacancies.<sup>13,14</sup> The BFO thin films can be thought as an n-type semiconductor due to the naturally produced oxygen vacancies that act as donor impurities.<sup>15</sup> Generally, the rectifying behavior in semiconductors comes from a p-n junction or a metal-semiconductor Schottky junction due to the existence of an energy barrier at the interface. In a ferroelectric capacitance, the metal-ferroelectric interfaces at the top and bottom electrodes would influence greatly the conduction because of the Schottky barriers. According to our results, the diodelike rectifying behavior is not observed in the virgin capacitance but appears in the poled sample and depends on the orientation of the polarization. This suggests that the energy barriers between n-type semiconducting BFO and metallic electrodes have been changed by the polarization switching.

Based on the analysis of our results, the switchable diode behavior in the BFO films can be explained qualitatively by the polarization modulation of Schottky-like barriers at both bottom and top electrodes. The ideal Schottky barrier at a metal-semiconductor interface can be determined by the difference of the metal work function and the semiconductor electron affinity. The work function of SRO is taken as 5.2 eV (Ref. 16) and the work function of Pt is about 5.3 eV. For BFO, the band gap  $E_g$  is 2.8 eV and the electron affinity  $\chi$  is 3.3 eV,<sup>17</sup> and then the work function of n-type BFO should be less than 4.7 eV. When BFO and SRO or Pt are joined, some of the electrons in the BFO should move spontaneously into SRO or Pt due to the higher Fermi level of BFO than that of SRO or Pt, and leave behind positive charges in BFO. Then depletion regions are formed by the positively charged regions in BFO near the bottom and top electrodes, respectively, and built-in fields are set up in opposite directions.

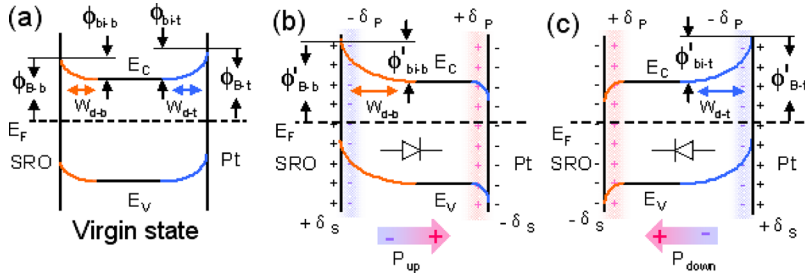


FIG. 4. (Color online) Schematic energy band diagrams illustrating the variations in Schottky barriers from back-to-back diodes at virgin (a) to a forward diode at polarized up (b) and a reverse diode at polarized down (c), corresponding to the I-V curves in Figs. 3(a)–3(c), respectively. Where,  $\phi_{B-b}$  ( $\phi_{B-t}$ ) is the Schottky barrier at bottom (top) interface;  $\delta_P$  is polarization charge;  $\delta_s$  is screen charge;  $w_{d-b}$  ( $w_{d-t}$ ) is the depletion width near bottom (top) electrode;  $\phi_{bi-b}$  ( $\phi_{bi-t}$ ) is built-in potential barrier near the electrodes.

The depletion regions or Schottky barriers might be modulated by the redistribution of charged impurities or carriers with ferroelectric switching. For a virgin BFO capacitance, at low electric field, the oxygen vacancies as donor impurities are not easy to move or release electrons, so the modulation of Schottky barriers could not happen by the as-grown polarized domains or polarization in the virgin state. By assuming no contribution from the as-grown polarization, the band structure of the virgin SRO/BFO/Pt capacitance at zero bias can be schematically plotted as shown in Fig. 4(a). The barrier heights in both interfaces are sufficiently large to inhibit Schottky emission from the metals into the semiconducting conduction band, so no matter the applied voltage is positive or negative, the virgin capacitance always works in high resistive state.

However, an enough high electric field is needed to pole the capacitance electrically or to switch the ferroelectric polarization. Under the high electric field, a neutral oxygen vacancy ( $V_O$ ) can release one or two electrons to conduction band and becomes positively charged ( $V_O^+$  or  $V_O^{2+}$ ), and moreover the polarization switching or domain wall movement may facilitate the movement of charged oxygen vacancies. For a polarized BFO thin film, the depolarization field can drive the released electrons to neutralize the positive bound charges at the surface and a narrow electron region can be formed near the surface with positive bound charges, resulting in the downward-bending of the band at this surface; meanwhile, near the surface with negative bound charges, neutral oxygen vacancies lose electrons become positive charged, resulting in the upward-bending of the band.<sup>2</sup> The opposite band variations give rise to the modulated Schottky barriers at the upper and lower interfaces. In addition, according to the model of metal-ferroelectric interface proposed by Pintilie and Alexe,<sup>10</sup> the variation in the built-in potential with ferroelectric polarization can be given by  $\Delta\phi_{bi}^p = \phi_{bi}' - \phi_{bi} = \pm P\delta/\epsilon_0\epsilon_s$ , where  $\phi_{bi}$  is the built-in potential without contribution from polarization,  $\phi_{bi}'$  is the built-in potential with contribution from polarization, the apparent  $\epsilon_0$  is the permittivity of free space,  $\epsilon_s$  is the static dielectric constant,  $P$  is ferroelectric polarization, and  $\delta$  is the thickness of a interface layer between the surface polarization charge and the metallic electrode. The value of  $\delta$  is estimated to be the order of a unit cell.<sup>18</sup> For our BFO films, the saturation polarization value is about  $60 \mu\text{C}/\text{cm}^2$ , and the measured low-frequency dielectric constant is about 50, then the variation in the built-in potential  $\Delta\phi_{bi}^p$  can be as high as 1.38 V for a  $\delta$  value of 1 nm. Figure 4(b) schematically shows the modulated band structure for the polarized up case at zero bias. In this case, at the lower interface between BFO and SRO, the built-in potential increases and the depletion region becomes wide, accompanied with upward band bending and an enhanced Schottky-like barrier; while at the upper inter-

face between BFO and Pt, the reverse phenomena occurs, where the band bending goes down and reaches an ohmic contact. So, in the polarized up case, the enhanced Schottky-like barrier at the lower interface plays a dominant role in the conduction thus the capacitance works as a forward diode. Figure 4(c) shows the band structure for the polarized down case at zero bias and the polarized down capacitance works as a reverse diode.

In conclusion, we have demonstrated the switchable diode effect in the epitaxial BFO thin films. By analyzing the work function of the materials, schematic energy band diagrams are set up to illustrate the variations in Schottky-like barriers from virgin state to electrically polarized up and polarized down states. The origin of the switchable diode effect is attributed to the modulation of Schottky-like barriers, which might be related to ferroelectric polarization, oxygen vacancies, electrode materials, etc.

This work was supported by the National Natural Science Foundation of China and the National Basic Research Program of China. The authors wish to thank Professor Y. G. Zhao and Mr. S. Zhang for their help in the measurement of ferroelectricity.

- <sup>1</sup>T. Choi, S. Lee, Y. J. Choi, V. Kiryukhin, and S.-W. Cheong, *Science* **324**, 63 (2009).
- <sup>2</sup>G. L. Yuan and J. Wang, *Appl. Phys. Lett.* **95**, 252904 (2009).
- <sup>3</sup>Y. Watanabe, *Phys. Rev. B* **81**, 195210 (2010).
- <sup>4</sup>P. W. M. Blom, R. M. Wolf, J. F. M. Cillessen, and M. P. C. M. Krijin, *Phys. Rev. Lett.* **73**, 2107 (1994).
- <sup>5</sup>H. Kohlstedt, A. Petraru, K. Szot, A. Rüdiger, P. Meuffels, H. Haselier, R. Waser, and V. Nagarajan, *Appl. Phys. Lett.* **92**, 062907 (2008).
- <sup>6</sup>C.-H. Yang, J. Seidel, S. Y. Kim, P. B. Rossen, P. Yu, M. Gajek, Y. H. Chu, W. Martin, M. B. Holcomb, Q. He, P. Maksymovych, N. Balke, S. V. Kalinin, A. P. Baddorf, S. R. Basu, M. L. Scullin, and R. Ramesh, *Nature Mater.* **8**, 485 (2009).
- <sup>7</sup>W. Wu, J. R. Guest, Y. Horibe, S. Park, T. Choi, S. W. Cheong, and M. Bode, *Phys. Rev. Lett.* **104**, 217601 (2010).
- <sup>8</sup>P. Maksymovych, S. Jesse, P. Yu, R. Ramesh, A. P. Baddorf, and S. V. Kalinin, *Science* **324**, 1421 (2009).
- <sup>9</sup>V. Garcia, S. Fusil, K. Bouzehouane, S. Enouz-Vedrenne, N. D. Mathur, A. Barthelemy, and M. Bibes, *Nature (London)* **460**, 81 (2009).
- <sup>10</sup>L. Pintilie and M. Alexe, *J. Appl. Phys.* **98**, 124103 (2005).
- <sup>11</sup>L. Pintilie and M. Alexe, *J. Appl. Phys.* **98**, 124104 (2005).
- <sup>12</sup>R. Meyer and R. Waser, *J. Appl. Phys.* **100**, 051611 (2006).
- <sup>13</sup>C. Wang, M. Takahashi, H. Fujino, X. Zhao, E. Kume, T. Horiuchi, and S. Sakai, *J. Appl. Phys.* **99**, 054104 (2006).
- <sup>14</sup>H. Yang, Y. Q. Wang, H. Wang, and Q. X. Jia, *Appl. Phys. Lett.* **96**, 012909 (2010).
- <sup>15</sup>S. R. Basu, L. W. Martin, Y. H. Chu, M. Gajek, R. Ramesh, R. C. Rai, X. Xu, and J. L. Musfeldt, *Appl. Phys. Lett.* **92**, 091905 (2008).
- <sup>16</sup>X. Fang and T. Kobayashi, *Appl. Phys. A: Mater. Sci. Process.* **69**, S587 (1999).
- <sup>17</sup>S. J. Clark and J. Robertson, *Appl. Phys. Lett.* **90**, 132903 (2007).
- <sup>18</sup>J. F. Scott, in *Ferroelectric Memories*, Advanced Microelectronics Series Vol. 3, edited by K. Itoh and T. Sakurai (Springer, Berlin, 2000).